

PAPER

Effect of process parameters on microstructure and wear resistance of niobium carbide coatings produced by pack cementation

To cite this article: Jin Zhang *et al* 2019 *Mater. Res. Express* **6** 096432

View the [article online](#) for updates and enhancements.



IOP | ebooks™

Bringing you innovative digital publishing with leading voices to create your essential collection of books in STEM research.

Start exploring the collection - download the first chapter of every title for free.



PAPER

Effect of process parameters on microstructure and wear resistance of niobium carbide coatings produced by pack cementation

RECEIVED
31 May 2019REVISED
1 July 2019ACCEPTED FOR PUBLICATION
11 July 2019PUBLISHED
19 July 2019Jin Zhang¹ , Shuai Li¹, Qinglian Sun¹, Pan Luo¹ and Yu Sun²¹ School of Materials Science and Engineering, Southwest Petroleum University, Chengdu 610500, People's Republic of China² School of Mechanical and Electrical Engineering, Southwest Petroleum University, Chengdu 610500, People's Republic of ChinaE-mail: jzhang@swpu.edu.cn

Keywords: niobium carbide coatings, orthogonal test, pack cementation

Abstract

The effects of the proportions of ferrocolumbium powder and ammonium chloride powder in the reaction medium, deposition temperatures, and deposition times on the thickness and mechanical properties of niobium carbide coatings were studied by means of orthogonal experiment. Mathematical analysis was conducted to quantify the influence of these four variables on the pack cementation process to obtain a superior production process with deposition temperature of 950 °C, deposition time of 5 h, proportion of ferrocolumbium powder at 20 wt%, and proportion of ammonium chloride at 5 wt%. The weight values of the experimental process parameters were 60.9% for deposition temperature, deposition time 37.4%, ammonium chloride powder 1.1%, and ferrocolumbium powder 3.1%. Further experiments were conducted with deposition temperatures set to 900 °C, 950 °C, and 1,000 °C, with coatings' surface microhardness of $925 \pm 60 \text{ HV}_{0.2}$, $860 \pm 30 \text{ HV}_{0.2}$, and $750 \pm 20 \text{ HV}_{0.2}$, respectively. Scanning Electron Microscope (SEM) surface morphology observation, X-ray diffraction (XRD) phase analysis, and grain size calculation showed that the surface phase of the three coatings all are NbC phases, and the grain size (37.0, 42.4, and 57.9 nm, respectively) increased with increasing temperature. The coatings' roughness decreased as temperature increased, and the 950 °C deposition temperature obtained the best wear resistance.

1. Introduction

Nowadays, one of the practical means to improve the service life of materials is surface modification [1–6], including techniques such as chemical vapor deposition [7], physical vapor deposition [6], electroless plating [8], thermal spraying, and electron-beam treatment [9, 10]. The equipment required for physical vapor deposition and chemical vapor deposition is too expensive, and the coating prepared by electroless plating has a poor bonding force. When surface modification is performed by thermal spraying, the modification process is not easy to control. A thermo-reactive powder-pack treatment, as a traditional process means, just makes up for the previously mentioned deficiencies. This technique is simple in process, convenient in operation, and has no additional harmful gas. It is an environmentally friendly process technology [11–15].

Niobium carbide coating is a high-temperature, wear-resistant coating that is often applied to the surface of high-temperature friction components. In addition, niobium carbide coatings have excellent hardness and toughness, as well as extremely high melting points [16]. The preparation of niobium carbide coatings by thermo-reactive deposition (TRD) technique not only has the advantages of low cost, mature technology, and excellent adhesion but also has little restriction on the shape of the substrate material. Therefore, many researchers have studied this technique. Researchers such as Reza Soltani and Cai [16, 17] obtained the growth kinetics formula of niobium carbide coatings on AISI L2 steel by controlling different deposition temperatures and times, finding that the coating would improve the wear resistance of the sample. Aghaie-Khafri *et al* [18] found that the thickness of niobium carbide coatings increased by pre-nitriding. Shan and other researchers [19, 20] found that rare earths can accelerate diffusion of carbon atoms. There are many studies on the

Table 1. Composition of substrate (wt%).

Content	C	Si	Mn	P	S	Cr
45 steel	0.45	0.25	0.15	0.03	0.03	0.15

Table 2. Test factors and their levels.

Factors	Levels			
A:Nb-Fe (wt%)	10	20	30	40
B: NH ₄ Cl (wt%)	3	5	7	9
C:temperature (°C)	860	900	950	1,000
D:Time (h)	4	4.5	5	6

preparation process of niobium carbide coatings, but most researchers use the control variable method to separate each process parameter and ignore the interaction between variables. Some studies [18, 21] indicate that the various process parameters would affect each other during the experiment.

In this research, orthogonal testing was used to design the orthogonal table, and the thickness of NbC coatings was used as the index. The relative importance of four factors—the proportions of ferrocolumbium powder and ammonium chloride in the reaction medium, deposition temperature, and deposition time—were finally obtained through numerical analysis. The weight of the experimental process parameters on the experimental results were numerically quantified. Subsequently, niobium carbide coatings were prepared under the process route derived from the normal price experiment, and the surface mechanics testing was carried out.

2. Experiment

The experimental substrate was 45 steel, with a composition as shown in table 1. First, the substrate is processed into a size of 50 × 15 × 5 mm, and metallographic sandpaper (ISO) of P400, P600, P800, P1000, and P1200 were used for grinding and polishing. Then the samples were ultrasonically cleaned with anhydrous ethanol, acetone, and deionized water for 10 min to remove the oil and impurities on the surface. Good surface condition could improve the quality of the formed coatings.

When TRD process was conducted, the reaction medium consisted of ferroniobium (64.9 wt% Nb, 34 wt% Fe) as master alloy, ammonium chloride (NH₄Cl) as an activator, and alumina (Al₂O₃) as an inert filler. In order to systematically study the influence of various process parameters on the thickness of the coating, an orthogonal test table of four factors and four levels was designed to determine the appropriate process route by using the reaction media of ferroniobium and ammonium chloride, the time, and the temperature of the heat treatment as variables. The experimental table is shown in table 2. After the experiment was completed, the samples were taken out and air cooled, and then the sample surfaces were cleaned with a damp cloth to smooth their surfaces.

For the cross-sectional morphology and thickness of niobium carbide coatings, the JSM-5600 scanning electron microscope was used for observation and measurement to determine the appropriate process parameters. For the coatings prepared under the orthogonal experimental optimization process, the phase composition of coatings was determined by DX-1000 X-ray diffractometer with Cu K α radiation. The scanning angle ranged from 10° to 80°, the length was 0.02°/step, and the scanning speed was 10° min⁻¹. The DHV-1000 microhardness tester was used to obtain the microhardness of coatings on 45 steel with a load of 20 gf kept for 10 s, and the Vickers hardness of each sample taken as an average of several measurements. The roughness test and wear experiments were measured by MFT-4000 sliding against GCr15 steel under the conditions of load of 30 N, sliding speed of 50 mm min⁻¹, and wear scar length of 5 mm. After wear experiments were finished, the worn surfaces of the samples were observed under a scanning electron microscope.

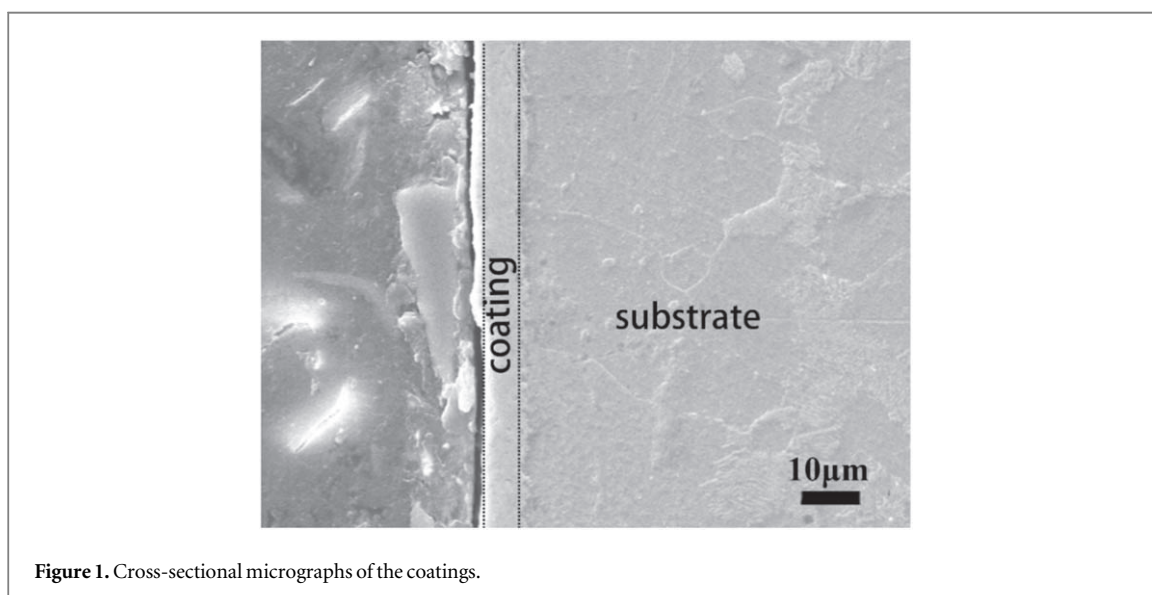
3. Experimental results and discussion

3.1. Orthogonal experimental results

The design principle of the orthogonal table is that each level of each factor meets each level of another factor only once and the experimental items after the combination of the variables are representative. There are many teaching materials and studies on the design of orthogonal experiments and orthogonal experimental tables [22]. An orthogonal table was designed as shown in table 3, and experiments were conducted according to the

Table 3. Orthogonal test table.

Factors	A (wt%)	B (wt%)	C (°C)	D (h)	Thickness (μm)
1	10	3	860	3	8.8
2	10	5	900	4	9.4
3	10	7	950	5	10.2
4	10	9	1,000	6	11.0
5	20	3	900	5	9.6
6	20	5	860	6	9.4
7	20	7	1,000	3	9.9
8	20	9	950	4	9.9
9	30	3	950	6	10.9
10	30	5	1,000	5	10.5
11	30	7	860	4	9.2
12	30	9	900	3	9.3
13	40	3	1,000	4	10.2
14	40	5	950	3	9.4
15	40	7	900	6	9.8
16	40	9	860	5	9.3

**Figure 1.** Cross-sectional micrographs of the coatings.

variables A , B , C , and D in the orthogonal table. The thickness of the prepared coatings was used as an experimental reference standard.

For the thickness measurement, the experiment uses the area method. By calculating the area of the coatings, and then dividing by the length of coatings, a reasonable thickness of coatings can be obtained. Figure 1 shows a cross-sectional view of a sample at deposition temperature of 900 °C for 5 h. It can be seen from the figure that the thickness of the coating, which has clear boundaries, is about 10 μm. Meanwhile, it is also found that the coatings are relatively flat and dense, and there are no obvious pores or defects at the joint of the substrate. In addition, figure 1 also shows a slit on the left side of the coating, which is due to the polishing residue of the inlay during the cross section preparation.

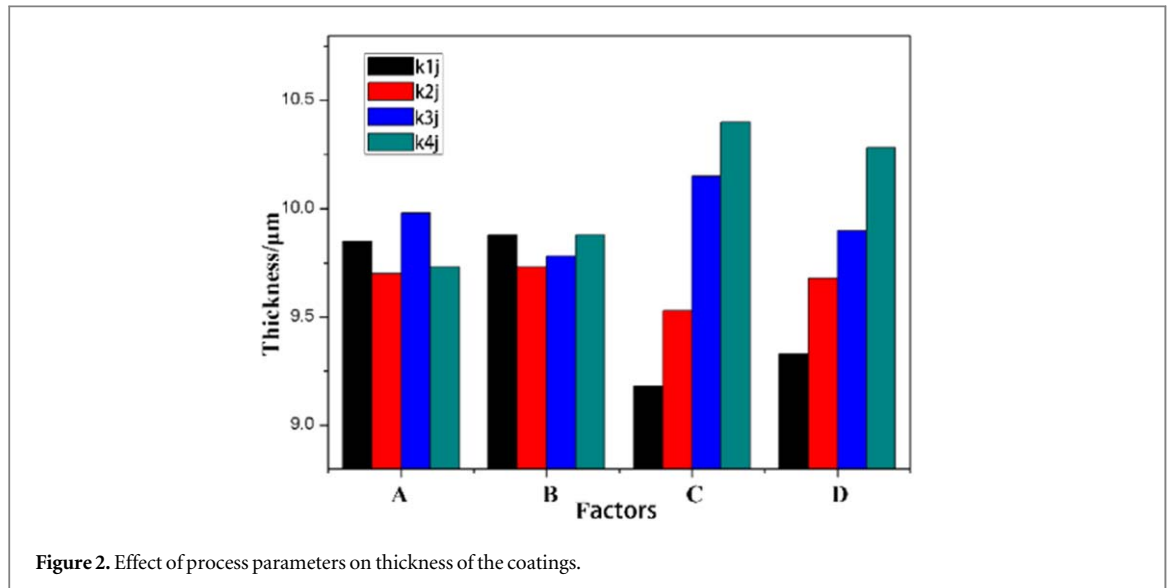
The orthogonal experimental table can be completed by calculating and registering the thickness, but table 3 cannot intuitively obtain the most suitable process route because mathematical processing is required. The specific process is as follows.

As shown in table 4, the orthogonal experimental table is further processed according to the results of the thickness of coatings in table 3. Among them, A , B , C , and D are different variables, and each variable corresponds to $K1j$, $K2j$, $K3j$, and $K4j$. Taking the values corresponding to A and $K1j$ as an example, it means the average of the sum of all coatings thicknesses at the first level of the A variable, and the value of R represents the range difference corresponding to each variable. And the larger the R value, the greater the weight of the variable.

Comparing the R values of each set of variables, the order of factors affecting the TRD process can be obtained. Therefore, it can be seen that: $C > D > A > B$, which means that the variable that best affects the

Table 4. Results of range analysis for the thickness values of the coatings.

Factors item	A	B	C	D
K1j	9.85	9.88	9.18	9.33
K2j	9.70	9.73	9.53	9.68
K3j	9.98	9.78	10.15	9.90
K4j	9.73	9.88	10.40	10.28
R	0.28	0.15	1.22	0.95

**Figure 2.** Effect of process parameters on thickness of the coatings.

TRD process is temperature, followed by heat treatment time, then the content of ferroniobium, and finally the content of ammonium chloride, which is consistent with the results of researchers such as Lin *et al* [23].

Figure 2 shows the distribution of process parameters to thickness, displaying the effect of each parameter on the thickness of coatings. At the same time, it can be concluded that the parameter of $A3B4C4D4$ is most likely to produce the thickest coating. Many researchers believe that the treatment temperature has the greatest influence on the thickness of coatings. However, it cannot generally be prepared at a fairly high deposition temperature and a fairly long deposition time because the cost would be prohibitive. Moreover, since the influence of the amount of the reaction medium is relatively small, a suitable process route is selected as $A1B1C3D3$. The high temperature will affect the mechanical properties of the substrate to a certain extent. However, although coatings with a larger thickness can be grown for a long time, the grain structure in the coating will also become larger. The reduction in micro-hardness, which in turn affects wear resistance, will be discussed in the next section. Using the orthogonal experimental table, not only the appropriate process route can be obtained, but also the variance value of each variable in the orthogonal experimental table can be acquired after the variance processing.

The statistical influence analysis (ANOVA) method is used to quantify the influence of each experimental variable. The results are shown in table 5, where F is the degree of freedom of each variable, and S represents the degree of quantification of each variable, which is derived from the following formula:

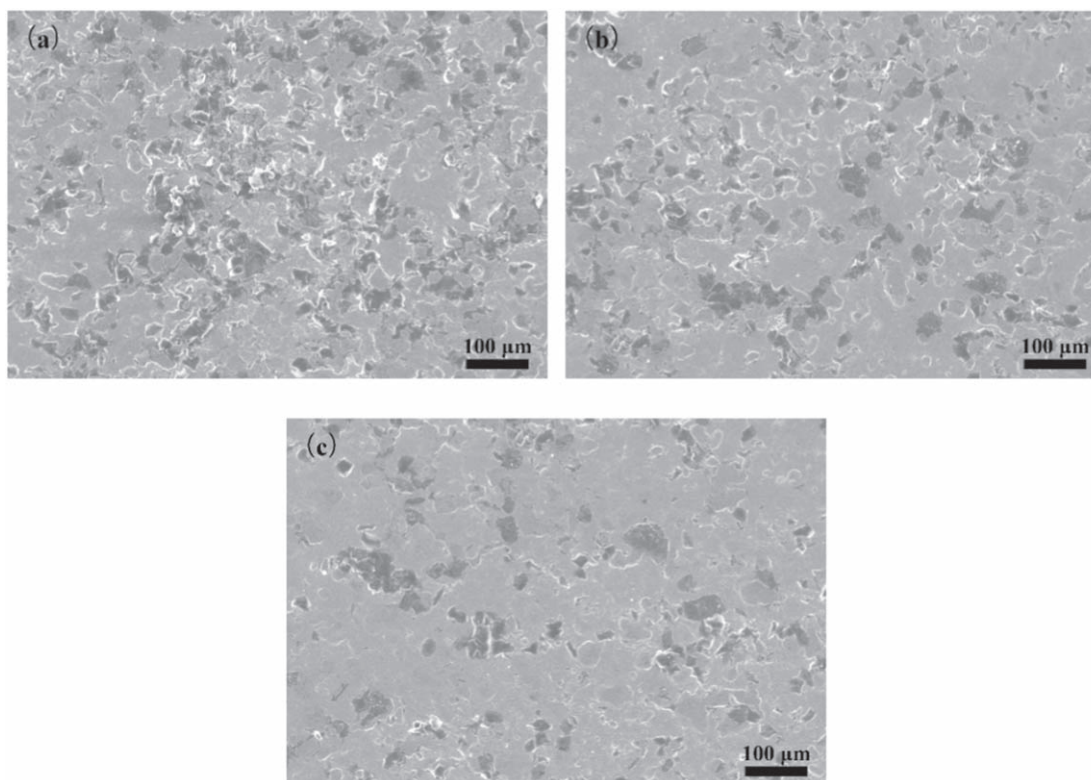
$$s = \frac{1}{(F + 1)} \sum_{i=1}^{F+1} (\bar{k}_{A_j} - k_{ij})^2 \quad (1)$$

From table 5, it can be seen that the temperature, represented by the letter C , has the largest influence on the thickness of coatings, and the weight is as high as 60.9%, followed by the time represented by the letter D accounting for 34.8%, the content of NbC powder represented by the letter A at 3.2%, and the content of the activator ammonium chloride represented by the letter B at 1.1%, which is due to the fact that during the process of TRD, the reaction medium is sufficient for the reaction process. Some studies even indicated that the reaction materials can be used repeatedly multiple times [24, 25].

For the process of coatings formation, the most decisive factor is the carbon activity of the matrix and the reaction time. The temperature and the elements in the matrix determine the carbon activity in the matrix, so

Table 5. Results of ANOVA for the thickness values of the coatings.

	Degree of quantification S	Degree of freedom F	Contributions (%)
A	0.0122	3	3.2
B	0.0043	3	1.1
C	0.2347	3	60.9
D	0.1339	3	34.8
Total	0.3851	12	100

**Figure 3.** SEM micrographs of niobium carbide coatings at different deposition temperatures: (a) 900 °C, 5 h; (b) 950 °C, 5 h; (c) 1,000 °C, 5 h.

that the heat treatment temperature and time can even be said to play a decisive role in the formation of niobium carbide coatings. For the discussion of the influence of different elements in the matrix, although some studies [26] have shown that some elements will reduce the activity of carbon, the impact on the performance and structure of the coatings requires more experiments to verify.

3.2. Characterization of coatings

After the orthogonal experiment, a suitable process route can be obtained. According to the selected process route, among the experimental process parameters, only the heat treatment temperature is changed, with values of 900 °C, 950 °C, and 1,000 °C, respectively, and the heat treatment time and the proportions of reaction media are kept unchanged. The reasons for choosing these temperature points is that these temperature points are currently in the temperature range used in factories for actual niobium carbide coating production and the values are the same as the orthogonal experimental temperature points.

Figure 3 shows the surface topography of the coatings at different temperatures. It can be seen that the coating surfaces were relatively rough, and there were pits and protrusions in some places. The reason for this phenomenon is attributable to the vacancy diffusion mechanism for the growth of coatings. The surface active Nb atoms diffuse downward, combine with the diffused C atoms from the matrix, and then produce the characteristic regions as shown in the original position. As can be seen from figures 3(a)–(c), the roughness of the surface of coatings decreases with the increase of the temperature. This is because, on the one hand, after the temperature rises, the defects such as micropores or cracks in the surface of coatings are melted and covered. On

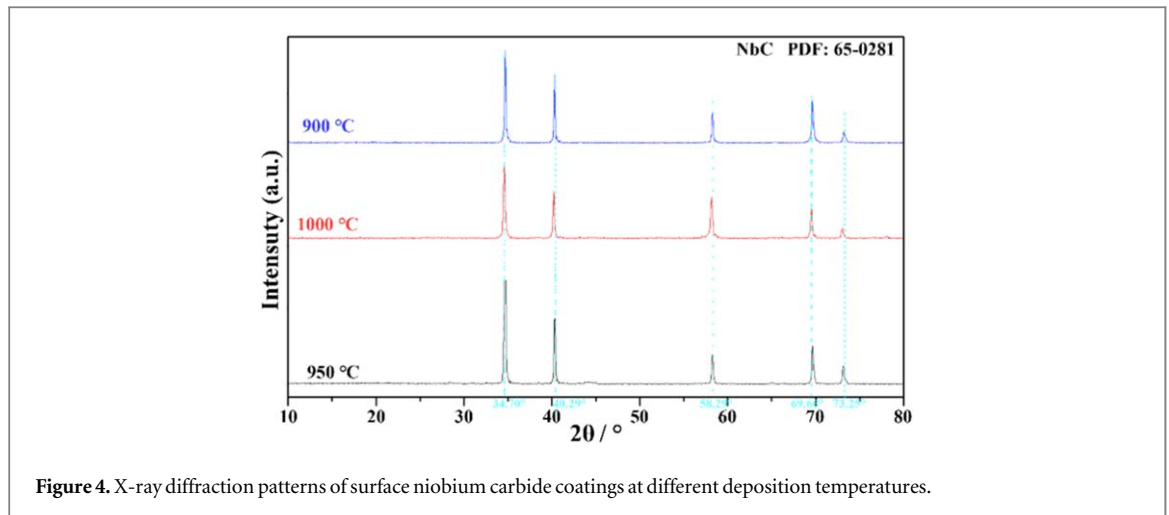


Figure 4. X-ray diffraction patterns of surface niobium carbide coatings at different deposition temperatures.

Table 6. Microhardness and roughness of the surface of coatings.

Deposition temperatures (°C)	900	950	1,000
Microhardness (HV _{0.2})	925 ± 60	860 ± 30	750 ± 20
Roughness (μm)	1.16 ± 0.12	1.05 ± 0.05	0.93 ± 0.03

Table 7. Grain size at three treatment temperatures.

Deposition temperatures (°C)	900	950	1,000
Grain size (nm)	37.0	42.4	57.9

the other hand, the speed at which the crystal grows becomes higher, the grain boundary becomes wider, and the number of grain boundaries within a certain area is reduced. The grain boundary position is prone to microcracks, and the microdefects of coatings are often generated at the interface of the grain boundary. Therefore, when the number of grain boundaries is reduced, the surface roughness of coatings is decreased.

X-ray diffraction, roughness tests, and hardness tests on the surface of coatings at different temperatures were carried out in order to verify the aforementioned ideas. The experimental results are shown in figure 4 and table 6. X-ray diffraction can be used not only to detect the phase but also to calculate the crystal grain width of the crystal from the x-ray spectrum. It can be seen from figure 4 that the phases of the coatings at different temperatures were NbC phases. By measuring and comparing the half-width of the diffraction peak, it can be concluded that the higher the temperature, the larger the grain size of the niobium carbide in coatings. In addition, according to the Scherrer equation,

$$D_{hkl} = Nd_{hkl} = \frac{K\lambda}{\beta_{hkl} \cos \theta} \quad (2)$$

In the formula, K is a constant, β is a half-height width of the diffraction peak, θ is an angle corresponding to the diffraction peak, and λ is a wavelength of the x-ray. Bringing the angle of a single diffraction peak into equation (2), the grain thickness of the corresponding crystal plane normal is obtained. After taking multiple angles into the calculation, the grain size D can be obtained by averaging. The calculation results of grain size at three treatment temperatures are summarized in table 7. It should be noted that the size of the grains in the material is not completely uniform. Because the grains may not be spherical and the thicknesses are different in diversity directions, it is required to take the grain thicknesses in a plurality of directions, which the average grain size is estimated according to. It can be seen from table 7 that the grain also increases as the temperature rises, which is consistent with the previous idea of the article.

Table 6 shows the microhardness and roughness of the surface of coatings under different temperature treatment conditions. The Ra value in the table represents the roughness of the surface of coatings, and the larger the value of Ra, the larger the roughness. It can be seen from the table 6 that the roughness of niobium carbide coatings decreases as the temperature rises. This may be attributed to the fact that as the temperature rises, the grain growth in coating is faster, and many small crystal grains are fused together into one large crystal grain, so that the number of the crystal grains in the coatings becomes small. At the macroscopic level, the coating appears

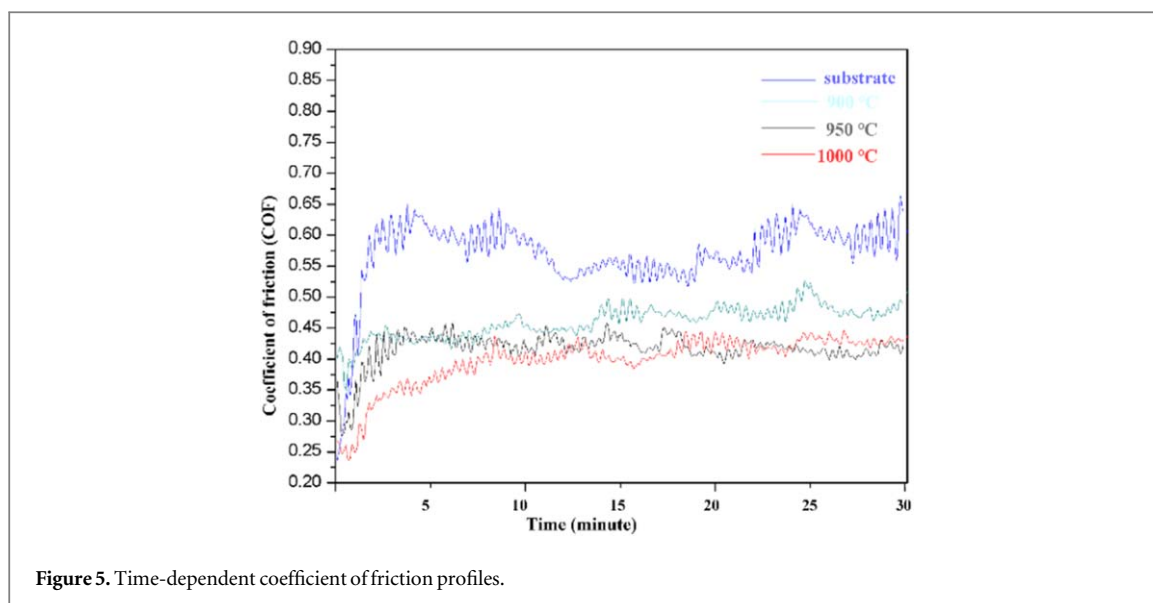


Figure 5. Time-dependent coefficient of friction profiles.

to be relatively flat and has a low the degree of fluctuation, which is consistent with the results of XRD pattern analysis and SEM observations. However, according to the theory of fine grain strengthening, the finer the crystal grains, the better the mechanical properties of the surface, so the hardness of the surface of the coating increases as the temperature decreases.

3.3. Wear test

Figure 5 shows the relationship between friction coefficient and time during the friction test of the substrate and coatings at three different processing temperatures. It can be seen that the substrate has the largest friction coefficient during the friction test. Within 10 min of the beginning of friction, the coefficient of friction varies widely. This is due to the initial stage of friction, the wear state is in the running-in period, and the grinding ball is just in contact with the surface of the sample. At this time, the grinding ball destroys the surface of the sample like a plough, so the friction coefficient changes greatly during the reciprocating motion of the grinding ball. The friction coefficient gradually decreases and stabilizes at around 0.55 in the following 10 min. At this moment, the friction is in a stable period and the wear state is relatively settled. On the one hand, the surface of the sample has formed a relatively mature wear scar band, so the grinding ball does not need to damage the surface of the sample again and can reciprocate smoothly on the formed wear scar band. On the other hand, due to the temperature rise at the contact point between the grinding ball and the wear band during the wear process, the friction contact surface can form an oxide film layer that has a friction-reducing effect, which is also a main reason for the reduction and stability of the friction coefficient. This wear condition then lasts for 10 min, and in the final stage of the friction and wear test, the coefficient of friction slowly rises to 0.65 at the end of the test, due to the fact that the wear scar and the oxide film, which originally have protective and antiwear effects, are destroyed again.

In addition, it can be seen from figure 6 that the samples with NbC coatings have lower friction coefficients during the rubbing process, indicating that NbC coatings have a certain anti-friction effect. At the same time, it is interesting to note that as the temperature of TRD process is increased, the reduction of friction coefficient for the coatings is not as good as possible. After the TRD temperature rises, the number of grain boundaries of coatings becomes small, the surface strength of coatings is weakened, and the antiwear effect of coatings is lowered. Therefore, the abrasion resistance of coatings deposited at 1,000 °C is not as good as those deposited at 950 °C. When the deposition temperature is relatively low at 900 °C, according to the microscopic morphology of the surface of NbC coatings (figure 3) and the roughness of the surface of NbC coatings (table 5), the number of the defects on NbC coatings is increased and the roughness becomes larger. The friction coefficient on the surface of NbC coatings is directly related to the surface topography of coatings. Therefore, the friction coefficient of NbC coatings at the other heat treatment temperatures is larger than that at 950 °C. For the comparison of the friction coefficients of coatings at the deposition temperature of 1,000 °C and 900 °C, it can be considered that the strength of the surface of coatings has a greater influence on the wear reduction effect than the roughness. Further research is needed on the factors affecting the wear resistance of NbC coatings.

Figure 6 shows the SEM micrograph of the scratch track of the substrate and coatings at three different processing temperatures. It shows that the wear of figure 6(d) is the most serious. It can even be seen that there are a lot of abrasive grains and debris on the surface, and some obvious scratches and furrows. Some abrasive particles and debris are pressed into and out of the wear band during the reciprocating grinding process. This is

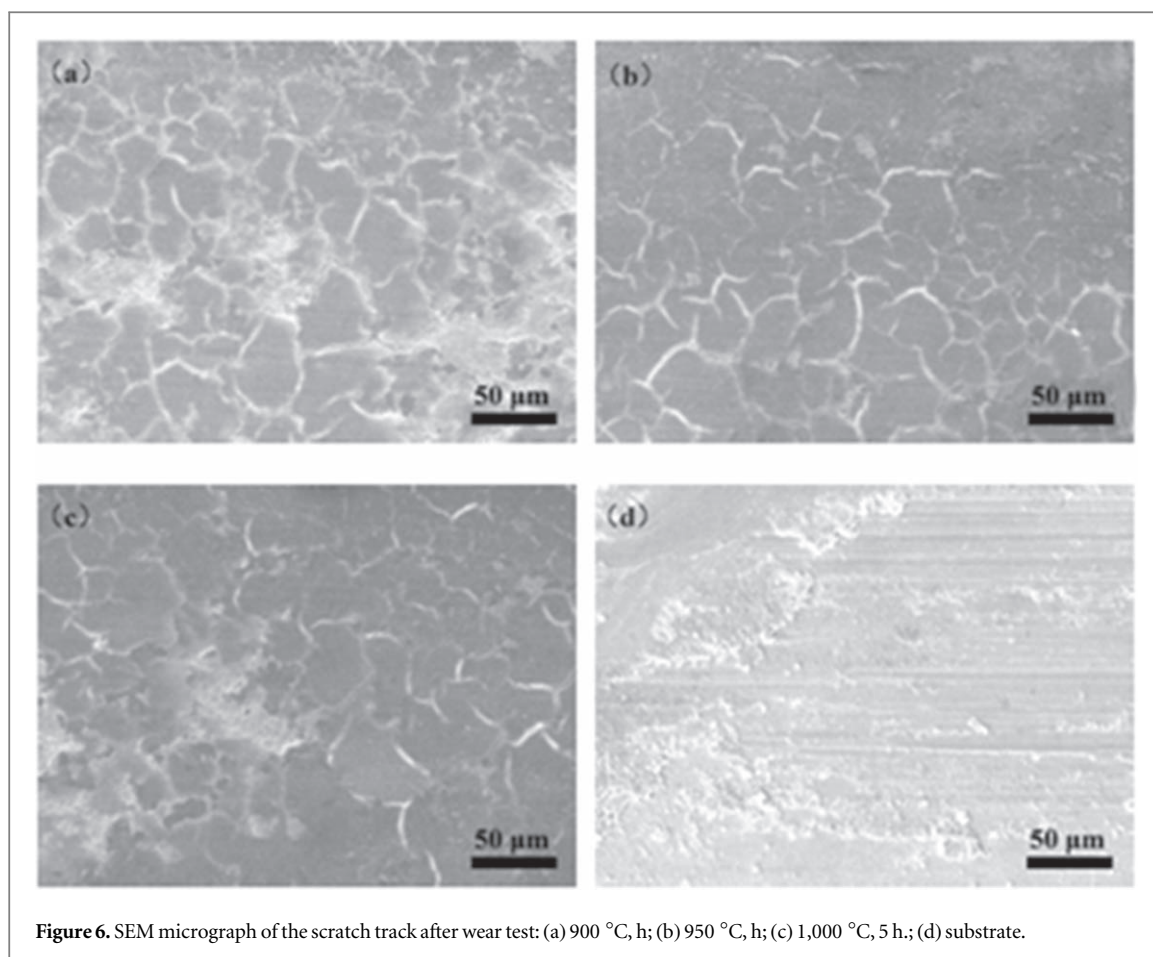


Figure 6. SEM micrograph of the scratch track after wear test: (a) 900 °C, 5 h; (b) 950 °C, 5 h; (c) 1,000 °C, 5 h; (d) substrate.

because during the wear process, the substrate and the grinding ball will continuously generate wear debris and abrasive grains. Hence, after the end of the friction test, a large amount of debris and abrasive grains can be observed on the surface. Because the grinding ball presses the existing abrasive grains and debris on the wear scar, and the grinding ball drives its relative base reciprocating motion, there are a lot of scratches and furrows on the surface of the substrate. The wear mechanism with these typical features is abrasive wear, which will cause a lot of material wear and tear in actual production.

Figures 6(a)–(c) show the surface topography of the scratch track at the deposition temperatures of 900 °C, 950 °C, and 1,000 °C, respectively. The images show that the wear scars of the as-prepared coatings are relatively light compared to figure 6(d), although there are still some scratches and microcracks on the surfaces. As can be seen from figures 6(a)–(c), however, the number and degree of damage of scratches and microcracks are greatly reduced. On the one hand, the surface micro-hardness of the niobium carbide coatings is relatively high compared with the substrate, and the coatings have the effect of abrasion resistance and wear reduction. On the other hand, the surface micro-hardness is related to the process of the powder-pack method. Since the temperature at which the active atoms permeate is around 900 °C, the carbon steel has been austenitized when the sample is heated to near this temperature point. After a certain period of heat preservation, the carbon steel has been completely austenitized. Because the sample is implemented by powder-pack method in an alumina crucible sealed with an alumina-based cement, it cannot be directly quenched, thereby causing the hardness of the substrate to decrease. In other words, the process of powder-pack method will act to soften the substrate. Therefore, the substrate has a certain tolerance to the vertical pressure of the grinding ball in the process of wear testing. As a consequence, in the process of reciprocating friction of the grinding ball, the surface of NbC coatings is not easily consumed, and the wear scar shows a slightly worn topographical feature.

Furthermore, it can be found from figures 6(a)–(c) that the wear surface has a few fine grinding debris and particles in addition to microcracks. In particular, it can be seen from figure 6(a) that a relatively large number of abrasive particles are present on the wear surface compared to figures 6(b) and (c). This is because the hardness of coatings is relatively higher and the roughness is comparatively larger, so coatings are likely to generate relatively more abrasive chips and particles in the friction test. For figure 6(c), because the hardness and roughness of coatings are relatively small, the surface of the coating is liable to generate microcracks and plastic

deformation regions. From this point of view, a wear pattern can be controlled by several wear mechanisms, and the wear scar mechanism in figures 6(a)–(c) is dominated by fatigue wear and abrasive wear.

Due to the high microhardness of the niobium carbide coatings, part of the coating is ground into fine third-body particles during the relative friction. Then, under the action of the third-body hard particles, the surface of the wear scar is easily furrowed; therefore, it is possible to see some wear debris and scratches. At the same time, due to the enhanced toughness of the substrate, the ability of the substrate to withstand the vertical pressure of the grinding ball becomes stronger. However, as the grinding ball reciprocates relative to the base body, the surface of the sample is prone to fatigue wear at this time, so plastic deformation and microcracking can be seen in the wear scar pattern. Comparing the wear scar surfaces at three deposition temperatures, it can be found that the wear resistance of coatings at the deposition temperature of 950 °C is better, and the surface wear is the lightest, which is also because the surface roughness and microhardness of coatings are both better for that sample.

4. Conclusions

According to the orthogonal experimental design, a suitable process route was obtained: the deposition temperature was 950 °C, the deposition time was 5 h, and a powder mixture consisted of 20 wt% Nb-Fe powder and 5 wt% NH₄Cl.

Calculated by variance calculation, the weight values of deposition temperature, deposition time, Nb-Fe powder, and activator on the powder process are calculated as 60.9%, 34.8%, 3.2%, and 1.1%, respectively.

It was found from X-ray diffraction and the Scherrer equation that the phase of coatings was NbC and the grain sizes of coatings at different deposition temperatures were calculated to be 37.0, 42.4, and 57.9 nm, respectively. The grain size of coatings was found to decrease as the deposition temperature increased. Scanning electron microscopy showed that the degree of fluctuation on the surface of coatings also decreased with the increase of deposition temperature, and this was verified in the roughness test. When deposition temperature was 900 °C, the roughness of surface coatings was the highest: $R_a = 1.16 \pm 0.12 \mu\text{m}$.

The surface microhardness of coatings at three different deposition temperatures of 900 °C, 950 °C, and 1,000 °C, was $925 \pm 60 \text{ HV}_{0.2}$, $860 \pm 30 \text{ HV}_{0.2}$, and $750 \pm 20 \text{ HV}_{0.2}$, respectively. The frictional experiments were carried out on the three coatings under the conditions of load of 30 N, sliding speed of 50 mm min⁻¹, and wear scar length of 5 mm. It was found that the wear resistance of coatings at the deposition temperature of 950 °C was the best.

ORCID iDs

Jin Zhang  <https://orcid.org/0000-0002-4643-3800>

References

- [1] Oliveira C K N, Benassi C L and Casteletti L C 2006 Evaluation of hard coatings obtained on AISI D2 steel by thermo-reactive deposition treatment *Surf. Coat. Technol.* **201** 1880–5
- [2] Pouraliakbar H, Khalaj G, Gomidzelovic L, Khalaj M and Nazerfakhari M 2015 Duplexceramic coating produced by low temperature thermo-reactive deposition and diffusion on the cold work tool steel substrate: thermodynamics, kinetics and modeling *Ceram. Int.* **41** 9350–60
- [3] Sen S 2005 A study on kinetics of CrxC-coated high-chromium steel by thermoreactive diffusion technique *Vacuum* **79** 63–70
- [4] Khafri M A and Fazlalipour F 2008 Vanadium carbide coatings on die steel deposited by the thermo-reactive diffusion technique *J. Phys. Chem. Solids* **69** 2465–70
- [5] Khalaj G and Khalaj M J 2014 Application of ANFIS for modeling of layer thickness of chromium carbonitride coating *Neural Comput. Applic.* **24** 685–94
- [6] Sen U 2004 Kinetics of niobium carbide coating produced on AISI 1040 steel by thermo-reactive deposition technique *Mat. Chem. Phys.* **86** 189–94
- [7] Miyake M, Hirooka Y, Imoto R and Sano T 1979 Chemical vapor deposition of niobium on graphite *Thin Solid Films* **63** 303–8
- [8] Rahman A and Jayaganthan R 2015 Effect of pH values on nanostructured Ni–P films *Appl. Nano.* **5** 493–8
- [9] Ivanov Y F, Alsarava K V, Gromov V E, Popova N A and Konovalov S V 2015 Fatigue life of silumin treated with a high-intensity pulsed electron beam *J. Surf. Investig.* **9** 1056–9
- [10] Zagulyaev D, Konovalov S, Gromov V, Glezer A, Ivanov Y and Sundeev R 2018 Structure and properties changes of Al-Si alloy treated by pulsed electron beam *Mater. Lett.* **229** 377–80
- [11] Fan X S, Yang Z G, Zhang C, Zhang Y D and Che H Q 2010 Evaluation of vanadium carbide coatings on AISI H13 obtained by thermo-reactive deposition/diffusion technique *Surf. Coat. Technol.* **205** 641–6
- [12] Castillejo F E, Olaya J J and Arroyo-Osorio J M 2014 NbcCr complex carbide coatings on AISI D2 steel produced by the TRD process *J. Braz. Soc. Mech. Sci. Eng.* **37** 87–92
- [13] Castillejo F E, Marulanda D M, Olaya J J and Alfonso J E 2014 Wear and corrosion resistance of niobium-chromium carbide coatings on AISI D2 produced through TRD *Surf. Coat. Technol.* **254** 104–11

- [14] Ghadi A, Soltanieh M, Saghafian H and Yang Z G 2016 Investigation of chromium and vanadium carbide composite coatings on CK45 steel by thermal reactive diffusion *Surf. Coat. Technol.* **289** 1–10
- [15] Biesuz M and Sglavo V M 2016 Chromium and vanadium carbide and nitride coatings obtained by TRD techniques on UNI 42CrMoS4 (AISI 4140) steel *Surf. Coat. Technol.* **286** 319–26
- [16] Cai X, Xu Y, Zhong L, Zhao N and Yan Y 2015 Kinetics of niobium carbide reinforced composite coating produced *in situ* *Vacuum* **119** 239–44
- [17] Soltani R, Sohi M H, Ansari M, Haghighi A, Ghasemi H M and Haftlang F 2017 Evaluation of niobium carbide coatings produced on AISI L2 steel via thermo-reactive diffusion technique *Vacuum* **146** 44–51
- [18] Aghaie-Khafri M and Fazlalipour F 2008 Kinetics of V(N,C) coating produced by a duplex surface treatment *Surf. Coat. Technol.* **202** 4107–13
- [19] Shan Z J, Pang Z G, Luo F Q and Wei F D 2012 Kinetics of V (N, C) and Nb (N, C) coatings produced by V–Nb–RE deposition technique *Surf. Coat. Technol.* **206** 4322–7
- [20] Liu X J, Wang H C and Li Y Y 2008 Effects of rare earths in borax salt bath immersion vanadium carbide coating process on steel substrate *Surf. Coat. Technol.* **202** 4788–92
- [21] Xiang Z D and Datta P K 2004 Pack aluminisation of low alloy steels at temperatures below 700 °C *Surf. Coat. Technol.* **184** 108–15
- [22] Diez C, Barrado E, Marinero P and Sanz M 2008 Orthogonal array optimization of a multiresidue method for cereal herbicides in soils *J. Chromatography A* **1180** 10–23
- [23] Lin N, Xie F, Wu X and Tian W 2011 Influence of process parameters on thickness and wear resistance of rare earth modified chromium coatings on P110 steel synthesized by pack cementation *J. Rare. Earth.* **29** 396–400
- [24] Liu X, Wang H, Li D and Wu Y 2006 Study on kinetics of carbide coating growth by thermal diffusion process *Surf. Coat. Technol.* **201** 2414–8
- [25] Bozza F, Bolelli G, Giolli C, Giorgetti A, Lusvarghi L, Sassatelli P and Thoma M 2014 Diffusion mechanisms and microstructure development in pack aluminizing of Ni-based alloys *Surf. Coat. Technol.* **239** 147–59
- [26] Loskutov V F, Khizhnyak V G and Pisarenko V N 1979 Vanadium carbide coating of tool steel surfaces *Steel In The USSR* **9** (7) 367–8
https://www.researchgate.net/publication/285756851_VANADIUM_CARBIDE_COATING_OF_TOOL_STEEL_SURFACES